Nuclear and magnetic order in the amorphous Tb_xCu_{1-x} system (0.18<or=x<or=0.65)

1991 J. Phys.: Condens. Matter 3 1985

(http://iopscience.iop.org/0953-8984/3/13/002)

J. Phys.: Condens. Matter 3 (1991) 1985–1994. Printed in the UK

Nuclear and magnetic order in the amorphous Tb_xCu_{1-x} system ($0.18 \leq x \leq 0.65$)

B Boucher†, M Sanquer†, R Tourbot† and R Bellissent‡

† Service de Physique du Solide et de Résonance Magnétique, Centre d'Etudes Nucléaires Saclay, 91191 Gif-sur-Yvette Cedex, France

‡ Laboratoire Léon Brillouin (CEA-CNRS), Centre d'Etudes Nucléaires Saclay, 91191 Gif-sur-Yvette Cedex, France

Received 9 July 1990, in final form 26 September 1990

Abstract. We have investigated the Tb_xCu_{1-x} ($0.18 \leq x \leq 0.65$) amorphous alloys by neutron diffraction both above and below the ordering temperature, determined the nuclear and magnetic short-range order and measured the magnetization in an intense applied field. We present a set of results showing the evolution with x of the distances between atoms, the coordination number and the local magnetization, and the magnetization dependence on field at low temperatures. We show also the evolution of the magnetization over a range from a few to few thousand ängströms.

1. Introduction

The amorphous alloys Tb_xCu_{1-x} ($0.18 \leq x \leq 0.65$) are formed from two different types of ion whose atomic size ratio is far from unity ($d_{Tb}/d_{Cu} \sim 1.4$) and can be easily obtained in amorphous state. Terbium has a large magnetic moment ($9\mu_B$) and a strong local anisotropy, which can result in a very characteristic asperomagnetic order. We have studied five concentrations $x = 0.18, 0.22, 0.33$, 0.50 and 0.65 for which the asymptotic Curie temperatures are positive.

In this paper, we present some results obtained by neutron diffraction measurement both above and below the magnetic ordering temperature and magnetization measurements in an intense applied field (up to 17 T).

Previous studies by small-angle neutron scattering (SANS) (Boucher 1980; Boucher *et al* 1983, 1986, 1987, 1988a,b,c, 1989b, 1990, Guimaraes *et al* 1987) have enabled us to obtain critical information in particular on the domain magnetization. These studies show also some heterogeneities of composition which generally do not have a strong influence on the determination of the short-range order as indicated in Chieux *et al* (1984). Thus, in the present work, we shall ignore these heterogeneities and discuss only the nuclear or magnetic order at short distances and the macroscopic magnetic behaviour.

From the set of experimental data we shall determine the evolution with the concentration x of parameters characteristic of nuclear and magnetic short range order and of magnetization for different sizes.

In section 2 we present the neutron diffraction measurements; their analysis and the results concerning the nuclear and magnetic ordering are presented in sections 3 and 4. Section 5 gives the results for classical magnetic measurements upon applied fields. The set of results is discussed in section 6.

0953-8984/91/131985+10$03.50

2. Experimental details

All samples have been produced by sputtering. The chemical analysis (Boucher *et al* 1983) shows for all samples both a weak dispersion of the nominal composition (about 2 at.%) and the presence of hydrogen, which is confirmed quantitatively by neutron scattering results and varies with x (table 1), of oxygen (about 1.2 at.%) and argon (1.2 at.%); these two latter impurities have little dependence on x.

Table 1. Ratio of the number of hydrogen atoms to the number of metallic atoms determined by chemical analysis and neutron scattering.

x	Chemical analysis	Neutron scattering
0.18	0.06	0.07
0.22	0.04	0.06
0.33	0.09	0.15
0.50	0.08	
0.65	0.09	0.10–0.11

For $x = 0.65$ a sample was prepared by planar flow casting for comparison with the sputtered sample† and was free of hydrogen. The neutron measurements were performed at Laboratoire Léon Brillouin, Saclay, France on the 7C2 diffractometer using two wavelengths ($\lambda = 1.106$ and 0.70 Å) and a multidetector of 124 × 124 cells.

The samples were either piled-up 20–50 μm sheets located perpendicular to the incident beam with a total thickness of 0.3 or 0.5 mm or finely ground powders put in a vanadium container 5 mm in diameter and 0.02 mm in thickness. The intensities were obtained on an absolute scale by normalization to a vanadium rod.

The low-temperature patterns were obtained in a cryostat for temperatures between 2.4 K and 300 K. From the difference between the low-temperature and high-temperature patterns, it has been possible to extract the magnetic scattering.

The magnetization measurements were performed at the SNCI Laboratoire L Néel (CNRS), Grenoble, France. The hysteresis loops were obtained by the usual extraction method with a field as high as 17 T for 1.7 K $\leq T \leq$ 300 K.

All experimental details and data analysis have been described earlier (Boucher *et al* 1989a). In particular the correction for paramagnetism and hydrogen has made it possible to determine the percentages of hydrogen and of the magnetic components of alloy using the method reported by Chieux *et al* (1984).

3. Neutron scattering at 300 K

The absolute intensity of neutron scattering patterns obtained at 300 and 5 K show a large scattering due to paramagnetism (300 K), frozen paramagnetic order (5 K), the presence of hydrogen in some samples and a large small-angle scattering. The hydrogen percentage determined from the incoherent part of the neutron scattering, reported in table 1, is in good agreement with the chemical analysis results.

† Sample prepared by J Bigot (Centre d'Etudes de Chimie Métallurgique (CNRS) CECM Vitry-sur-Seine, France)).

The $S(Q)$ structure factor and the Fourier transform (FT) are showed in figures 1 and 2. At low q-values we observe (figure 1) a small pre-peak located at about 1.24 Å followed by two intense rings (see also table 2). The pre-peak seems to stay at the same position and to be always very weak irrespective of x. It is impossible to measure its parameters, only its existence is not in doubt. The meaning of this pre-peak which tends to increase in size when the magnetic ordering appears, is not clear. Both size effect (Bletry 1978) and chemical short-range order have been invoked to explain this pre-peak (Chieux and Ruppersberg 1980). However, there is no strong experimental evidence to support the validity of either explanation. When x increases (the proportion of the large Tb ions increases), the first peak tends to move towards the origin owing to an increase in the number of Tb–Tb pairs.

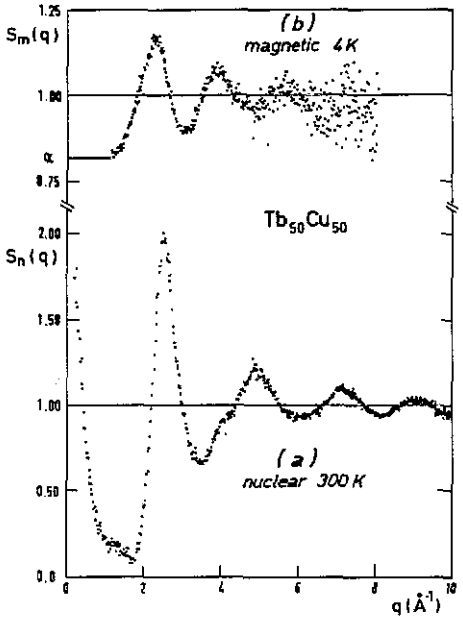

Figure 1. $Tb_{50}Cu_{50}$. (*a*) Nuclear structure factor $S_n(q)$ for a pattern taken at 300 K. The pre-peak is indicated by P above an arrow; on the left-hand side, SANS is shown. (*b*) Magnetic structure factor, corrected for the magnetic form factor i.e. $f(1/f^2)S(q)$. $S_m(q)$ corresponds to the difference between patterns taken at 4 and 300 K, the spectra being corrected for paramagnetism and hydrogen scattering and normalized to the large q scattering. The magnetic SANS has been suppressed.

The only difference between the quenched and the sputtered samples is that the oscillations of the scattered intensities are a little larger and narrower for the quenched sample, especially the first peak. This is also true for magnetic scattering at low temperatures, which indicates a little more ordered state for the quenched sample, but the differences are so weak that the FT indicate a difference only for magnetic scattering.

For 2 Å $< r <$ 4 Å the FT (figure 2) shows a wide peak which can be deconvoluted in three peaks centred on distances observed in crystalline solids: Cu–Cu, about 2.6 Å; Cu–Tb, about 3.00 Å; Tb–Tb, 3.6 Å. It is not possible to determine the coordination numbers of a diatomic sample, without making assumption (curve shape, interatomic distances, etc). Thus the FT curve has been assumed to be the sum of three Gaussians

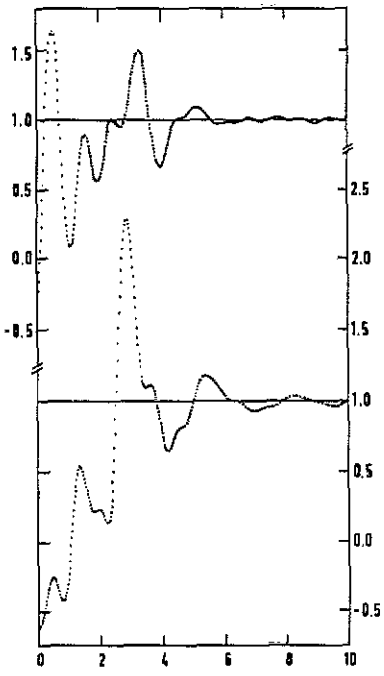

Figure 2. Pair correlation functions: FT transforms of (*a*) $S_m(q)$, and (*b*) $(1/f^2)S_m(q)$. In order to give the reader an idea of the uncertainties, we have shown all the cut-off oscillations which are, of course, without any physical meaning for $r < 2$ Å. These oscillations of $g(r)$ are much higher at low T owing to the very low precision at high q of the structure factor (see figure 1), which results from the extremely low value of the magnetic form factor.

Table 2. Position and intensity of the first two peaks and pre-peak for the $S(q)$ pattern.

	Prepeak		First peak		Second peak	
x	Position q (Å^{-1})	Intensity	Position q (Å^{-1})	Intensity	Position q (Å^{-1})	Intensity
0.18	1.237	0.122	2.99	2.38	4.95	1.24
0.22	1.35		2.90			
0.33	1.18	0.125	2.67	2.08	4.81	1.37
0.50	1.237	0.168	2.50	2.00	4.88	1.26
0.65 quenched sample			2.40	2.39	4.12	1.18
0.65 sputtered sample			2.42	2.08	4.00	1.12

whose integration lead to a coordination number which has to be weighted by the concentration and scattering length factor. For the fit all parameters were free to vary. The resulting FWMH (figure 3) are slightly different from one another but all of them are close to 0.4 Å which corresponds to a 10 Å cut-off. Thus the true width may be assumed to be smaller than 0.4. Table 3 gives the results with adjustable distances for the fit and the number of neighbors for a statistical distribution. The latter has been determined using the calculation of Schütte and van der Waerden (1951) for an alloy with two kinds of atom in contact with diameters d_1 and d_2. We point out

that the experimental values are close to the statistical distribution. Copper seems to present a small tendency to heterobonding, contrary to terbium which tends to surround itself with terbium. However, it is necessary to view the results cautiously because the deconvolution problem is not simple and the reliability depends on the accuracy of assumptions. So errors in the fitting routine are quite difficult to estimate accurately as they come not only from the fitting procedure itself but also from the uncertainties in the FT. However, 15% of the Gaussian width and 2 or 3% of the positions should be reasonable estimates of the errors of the procedure.

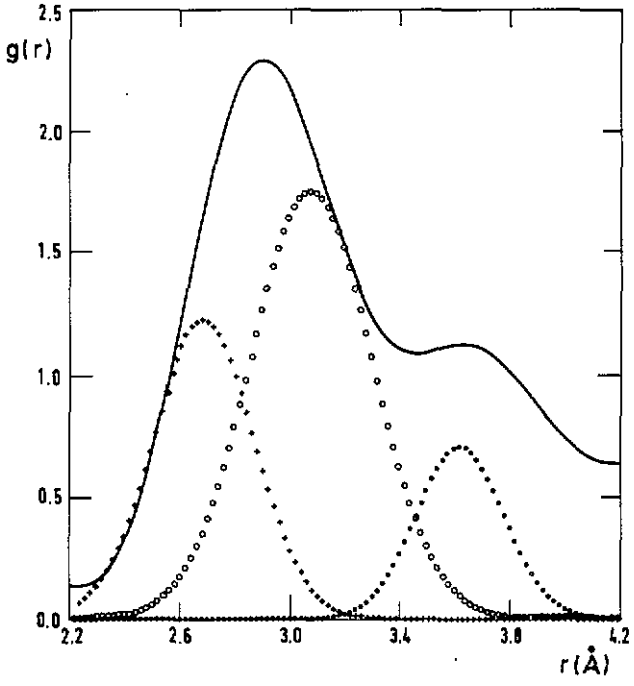

Figure 3. Deconvolution into three Gaussians of the first peak of the pair correlation function.

4. Neutron scattering at low temperatures (1.4 K $\leq T \leq$ 8 K)

A magnetic ordering temperature can be defined as the temperature at which some coherent magnetic scattered intensity appears in the form of diffusion rings while the incoherent paramagnetic scattering decreases and an intense small-angle magnetic scattering is observed. This temperature is dependent on x and is of order of 2Θ, Θ being the asymptotic Curie temperature (table 2). The magnetic scattering can be obtained as the difference of the low- and high-temperature patterns. Figure 1(*b*) shows the magnetic structure factor.

It has been shown by Blech and Averbach (1964) and Wright (1980) that, due to the angular correlation of the magnetic moments, the structure factor not only varies as $1/qr$ but also exhibits an additional term involving both $1/q^2r^2$ and $1/q^3r^3$ dependences. In the case of rare earths the smallest values of the magnetic ion pair distances (about 3.6 Å) lead to an order of magnitude less for this additional term. Moreover,

Table 3. Characteristic values (distance and coordination) of nuclear order. d_i is the distance deduced from three Gaussian fit of the first $g(r)$ peak (figure 3). Stat., statistical distribution; Exp., experimental distribution; XR, x-rays; N, neutrons.

				Coordination number							
	Distance			Cu–Cu		Cu–Tb		Tb–Cu		Tb–Tb	
x	d_1 (Å)	d_2 (Å)	d_3 (Å)	Stat.	Exp.	Stat.	Exp.	Stat.	Exp.	Stat.	Exp.
0.18	2.58	3.08	3.56	9.1	8.58	2.0	3.10	12.4	14.15	2.6	3.88
0.22[a], XR	2.50	2.98	3.5	8.5	8.2	2.4	3.0	11.7	10.7	3.3	4.2
0.22, N	2.52	2.96	3.56		5.1		4.35		15.5		10.5
					5.9		3.7		13.0		5.9
0.33	2.62	3.0	3.60	6.8	6.66	3.4	3.86	9.7	7.84	4.8	5.80
			3.56		6.68		3.84		7.80		5.76
0.50	2.60	3.08	3.60	4.7	3.9	4.7	4.8	7.0	4.8	7.0	6.7
0.65[b]	2.40	2.94	3.51	3.1	$\simeq$1	5.6	5.3	4.7	3.0	8.8	9.8

[a] After Chieux *et al* (1984).
[b] After Boucher *et al* (1989a).

in this type of alloy, no correlation between easy-magnetization axes and radius vector has been observed and no theoretical argument can be advanced to suggest such correlations; following Wright the extra term due to the directional properties of moments is, if not zero, at least much smaller than the $1/qr$ term and can be neglected. In this case, a one dimensional FT of the magnetic cross section is possible.

The corresponding FT exhibits a peak centred on the first nearest Tb–Tb distance, indicating non-zero local magnetization (figure 2). The simultaneous existence of this peak in the FT and of small-angle scattering in the structure factor suggest the presence of asperomagnetic order. From the area of the magnetic peak of the FT, it is possible to obtain a magnetic coordination number defined, following normalization to scattering by one Tb atom moment, as the effective number N_M of atoms carrying a full moment ($9\mu_B$) and aligned in the same direction. We can deduce from the ratio $N_M/N_N(=\cos^2\varphi)$, where N_N is the nuclear coordination number, and φ is the mean angle between the first neighbours and the central atom. Then we obtain the mean value of the magnetization M_1 for the first-neighbour shell of an atom. For $q \simeq 1$ Å^{-1}, we observe a minimum α of $S_m(q)$ for every x-value. This minimum corresponds to the maximum value of the magnetically disordered part and its complement $1-\alpha$ to the minimum of the ordered magnetic part. Thus we can say that $(1-\alpha)M^2$ is a minimum value of the magnetization where M is the magnetic moment per Tb atom. This minimum is seen for $q \simeq 1$ Å^{-1}, e.g. for a sphere of approximate radius 6 Å and corresponds to three or four shells.

Thus we have the magnetization values M_1 and M_2, respectively, for the first neighbour and for a volume corresponding to about 10 Å linear size (next three to four shells). We shall see in the next section that it is possible to give a good approximation of the domain magnetization M_D. Thus the magnetic order can be described by the magnetization values on three different scales, 3 Å (nearest neighbours), 10 Å (next three to four shells) and 10^3 Å (domains). It is possible, irrespective of the value of x, to measure α and to deduce M_2; however, for the two smallest x-values it was impossible to determine N_M, the magnetic intensities of rings being too small.

The magnetization between first neighbours is observed to be large (about (6–7)μ_B/Tb atom) (table 4) with a relatively weak mean dispersion (35–50°) and only

a weak dependence on x for high x-values (for low x-values ($x \leq 0.22$) it cannot be determined).

Table 4. Characteristic values (distance and effective coordination number) of magnetic order: N_N is the nuclear coordination number for the experimental distribution; N_M is the effective magnetic coordination number; φ is the mean dispersion of first-neighbour moments; M_1 is the magnetization of first neighbours, M_2 is the magnetization of the first three shells.

x	d Tb–Tb	N_N (exp.)	N_M	cos φ	φ (deg)	M_1 (μ_B/Tb atom)	α	M_2 (μ_B/Tb atom)
0.18	3.56	3.86	—			—	0.978	1.32
0.22[a]	3.56	10.5–5.9	—			—	0.951 0.913	2–2.65
0.33	3.60	5.8	3.85	0.815	35.0	7.3	0.875	3.18
0.50	3.60	6.7	4.6	0.828	34.0	7.3	0.74	4.6
0.65[b]	3.51	9.8	6.6	0.820	35.0	7.3	0.65	5.3
0.65[c]	3.51	9.8	4.4	0.670	48.0	6.0	0.78	4.2

[a] After Boucher *et al* (1986).
[b] Quenched sample.
[c] Sputtered sample.

Irrespective of the value of x, the magnetic oscillation amplitudes decrease with increasing temperature and disappear at temperatures much higher than Θ (asymptotic Curie temperature, (table 5)). For example, for $x = 0.65$, Θ is 90 or 58 K depending on the preparation process of the sample (quenched or sputtered) while the magnetic oscillations disappear for both samples at 150 K (Boucher *et al* 1989a). Thus these temperatures are representative of different scales: one for the magnetic short-range order (a few interatomic distances), and the other for macroscopic behaviour.

Table 5. Characteristic magnetic values at constant temperature. Θ is the asymptotic Curie temperature; M_r is the remanent magnetization; H_C is the coercive field; E_L is the energy of the full hysteresis loop; β is the coefficient of the saturation approach law ($M = M_S(1 - \beta/\sqrt{H})$. M_1 and M_2 are magnetizations of the first and first 3-shell neighbours respectively; M_D is the magnetization of a domain.

Sample x	(K)	Θ (K)	M_r (emu g^{-1})	M_r (μ_B/Tb atom)	H_c (T)	E_L (erg g^{-1})	β (Oe$^{1/2}$)	M_1 (μ_B/Tb atom)	M_2 (μ_B/Tb atom)	M_d (μ_B/Tb atom)
0.65[a]	1.4	90	115	4.0						
0.65[a]	4		106	3.67	1.7	7×10^6	86.25	7.0	5.3	
0.65[a]	7		100	3.45		5×10^6	78.21			3.8
0.65[b]	1.4	58	60	2.0	0.7	4×10^6	121.6	6.0	4.2	
0.50	1.4	56	60	2.4		3.3×10^6	111.47			
0.50	4		30	1.2	0.4	1×10^6		65.2	4.6	3.0
0.33	8	23	10	0.5	0.17	5×10^5		7.3	3.18	0.9
0.22	5	17					90.48		2.12–2.6	
0.18	5	$\simeq$1								

[a] Quenched sample.
[b] Sputtered sample.

5. Magnetic behaviour

For illustration, hysteresis loops of sputtered $Tb_{65}Cu_{35}$ at 1.4 and of quenched at $Tb_{65}Cu_{35}$, at 4 K are represented in figure 4 and characteristic parameters for all x-values are given in table 5. Hysteresis loops are characterized by the following.

(i) A saturation approach as $M = M_S(1 - \beta/\sqrt{H})$ for all alloys whatever x (M_S being the saturation magnetization): because of the small range of H (10–17 T) for which this law is obeyed, it is not possible to determine the high-field susceptibility; for the same x-values, the quenched sample is less difficult to saturate (β smaller) than the sputtered sample.

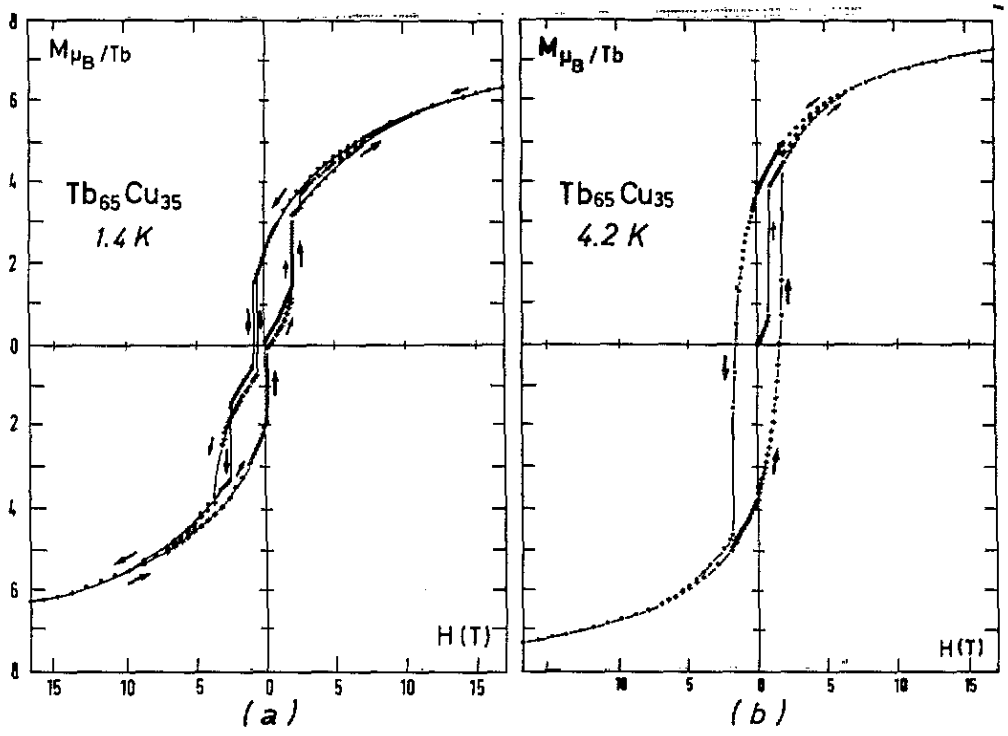

Figure 4. (*a*) Sputtered $Tb_{65}Cu_{35}$ hysteresis loops at 1.4 K and (*b*) quenched sample at 4 K. At very low temperatures the magnetic after-effect becomes important and distorts the loop.

(ii) A strong local anisotropy; if we write, as Cornelison and Sellmyer (1984), that $K = \frac{3}{2}\int_{M_R}^{M_S} H\ dM$ (M_S and M_R being the saturation and remanent magnetization values), we are led to very similar values of K irrespective of x; however, the integral is not convergent with a $H^{-1/2}$ law. We can only emphasize, considering the β-values, that the K-values are at least few 10^8 erg cm^{-3}, much larger than the values suggested by Cornelison and Sellmyer (1984) for REGaFe and at least of the same order as those proposed for REAg (Boucher 1977a).

(iii) An energy corresponding to the hysteresis loop at 4 K of the order of 10^6 erg g^{-1} depending on sample composition: this energy is of the same order of energy found for $Tb_{52}Ag_{48}$ (Boucher 1977b). A field as high as 10–12 T is needed to reach the loop saturation

(iv) A relatively weak coercive field H_c (for which the magnetization is inversed): for $H \gtrsim H_c$ the magnetic order is relatively unstable (magnetization jumps due to a magnetic after effect) as already observed in severals alloys, e.g. DyCu (Coey *et al* 1981) and TbSi (Simonnin *et al* 1986). This instability is more or less marked depending on the temperature and composition (figure 4) and the preparation process. The after-effect is more important in the sputtered sample which is also less ordered (Boucher *et al* 1989a, b).

(v) A remanence magnetization M_R clearly smaller than $M_S/2$: this magnetization corresponds to the sum of domain magnetizations in zero field when the magnetizations have been oriented by a high field. For the quenched $x = 0.65$ sample, we have been able to measure the SANS for a sample cooled in an applied field and to determine the dispersion of domain magnetization when the field has been relaxed (Boucher *et al* 1988c); we have obtained, in this way, a domain magnetization value $M_d = M_r/\cos\phi$, ϕ being the mean dispersion angle of domain magnetizations. In the absence of information on applied-field SANS, we can approach the domain magnetization value from the viewpoint of the values of the contrast for non magnetic 'bubbles' (in a 'seedy magnetic' model). That is the case for $x = 0.33$ or 0.50 (Guimaraes *et al* 1987). This value is a maximum because it corresponds to value around the bubbles and not taken over the whole domain. Alternatively the contrast between large domains deduced from SANS measurements allows us to have a minimum value only, and we are certain that this value is much too weak. Whatever it may be, we remark that domain magnetization varies as x between $4\mu_B$ and $0.5\mu_B$ per Tb atom. Thus for every sample we are able to give three values of magnetization corresponding to the three different scales of 3, 10 and 10^3 Å. Table 5 summarizes all the results.

6. Discussions

The study of Tb_xCu_{1-x} leads to the following general results for all values of x.

(i) The first neighbours of an atom consist of two kinds of atom in proportions close to the statistical distribution; only a light tendency towards heterobonding has been observed.

(ii) The preparation process does not result in spectacular properties. The most striking fact is the scattering by hydrogen for the sputtered samples. We observe a tendency towards a more ordered state in quenched samples, irrespective of the temperature.

(iii) At low temperatures, all samples present an asperomagnetic structure with $\Theta > 0$; the local magnetization decreases with distance. The dispersion of the first magnetic moments is much weaker than that expected for a random distribution, indicating that the exchange predominates over local anisotropy or that the easy-magnetization direction is correlated. For third neighbours, the moments are more dispersed (greater than 55°) and in spite of that the domains present a noticeable magnetization.

(iv) The remanent magnetization, coercive field and energy of the hysteresis loop decrease with increasing x in the range studied of about an order of magnitude. These parameters are almost of the same order as those for $Tb_{52}Ag_{48}$ (Boucher 1977a, b).

The Tb-rich alloys ($x \geq 0.50$) show hysteresis loops whose shape can be identified with the loops predicted by Callen *et al* (1977) for local random anisotropy (LRA) of

the same order as exchange. The LRA constant is clearly higher than that determined by Cornelison and Sellmyer (1984) for REGaFe alloys. This tends to indicate that in these Tb-rich alloys the exchange and the local anisotropy are of the same order and of high level. For low x-values the loops are smoother and correspond to a smaller energy for alloys in which the LRA is of the same order as in the preceeding case and the exchange is probably less intense owing to the larger dilution.

The $H^{-1/2}$ law has been predicted by Chudnovsky and Serota (1983) but only for weak LRA. However, for Tb_xCu_{1-x} amorphous alloys, this law is observed irrespective of the value of x and with a LRA of the same order as the exchange. The fact that all alloys obey the $H^{-1/2}$ law seems to show that this approach to saturation can also exist with a large anisotropy.

In conclusion, it can be said that we do not observe any qualitative difference between nuclear and/or magnetic order, and the magnetic behaviour of the different samples irrespective of the preparation processes or compositions. Only a variation in the magnitude of different parameters with x is found.

Acknowledgments

The authors wish to thank to Dr J C Picoche and M Guillot (SNCI (CNRS), Grenoble France) for their help with the high-field magnetization measurements and Dr Menelle and J P Ambroise (Laboratoire Léon Brillouin (CEA-CNRS), Centre d'Etudes Nucléaires de Saclay) for their assistance with the neutron measurements.

References

Blech I A and Averbach B L 1964 *Physics* **1** 31
Bletry J 1978 *Z Naturf.* a **33** 327–43
Boucher B 1977a *IEEE Trans. Mag.* **MAG-13** 1601
—— 1977b *Phys. Status Solidi* (a) **40** 197
—— 1980 *J. Physique Coll.* **41** C8 135
Boucher B, Chieux P, Convert P, Tourbot R and Tournarie M 1986 *J. Phys. F: Met. Phys.* **16** 1821
Boucher B, Chieux P, Convert P and Tournarie M 1983 *J. Phys. F: Met. Phys.* **13** 1339
Boucher B, Chieux P, Sanquer M and Tourbot R 1990 *J. Non-Cryst. Solids* **117–118** 191
Boucher B, El Gadi M, Sanquer M, Tourbot R and Bellissent R 1989a *J. Phys.: Condens. Matter* **1** 2057
Boucher B, El Gadi M, Sanquer M, Tourbot R, Bigot J, Chieux P, Convert P and Bellissent-Funel M C 1988a *Z. Phys. Chem., NF* **157** 23
Boucher B, Sanquer M, Tourbot R and Chieux P 1988c *J. Physique Coll.* **49** C8 1727
Boucher B, Sanquer M, Tourbot R, Chieux P, Convert P, Maret M and Bigot J 1988b *Mater. Sci. Eng.* **99** 161
Boucher B, Sanquer M, Tourbot R, Chieux P and Maret M 1989b *J. Phys.: Condens. Matter* **1** 2647
Callen E, Liu Y J and Cullen J R 1977 *Phys. Rev.* B **16** 263
Chieux P, de Kouchkovsky R and Boucher B 1984 *J. Phys. F: Met. Phys.* **14** 2239
Chieux P and Ruppersberg H 1980 *J. Physique* **41** C8 145
Chudnovsky E M and Serota R A 1983 *J. Phys. C: Solid State Phys.* **16** 4181
Coey J M D, McGuire T R and Tissier B 1981 *Phys. Rev.* 24 1261
Cornelison S G and Sellmyer D J 1984 *Phys. Rev.* B **30** 2845
Guimaraes D, Sanquer M, Tourbot R, Bellissent-Funel M C and Boucher B 1987 *Magnetic Properties of Amorphous Metals* ed A Hernandez, V Madurga, M C Sanchez-Trujillo and M Varquez (Amsterdam: Elsevier) p 77
Schütte K and Van der Waerden B 1951 *Math. Ann.* **23** 96
Simonnin P, Tourbot R, Boucher B, Perrin M and Vanhaute J 1986 *Phys. Status Solidi* (a) **98** 551
Wright A C 1980 *J. Non-Cryst. Solids* **40** 325